# Sleep Spindle Detection and Prediction Using a Mixture of Time Series and Chaotic Features

*Amin HEKMATMANESH*[1], *Mohammad MIKAEILI*[2], *Khosrow SADEGHNIIAT-HAGHIGHI*[3], *Huapeng WU*[1], *Heikki HANDROOS*[1], *Radek MARTINEK*[4], *Homer NAZERAN*[5]

[1]Laboratory of Intelligent Machines and Sleep Center, Department of Energy, Lappeenranta University of Technology, Skinnarilankatu 34, 53850 Lappeenranta, Finland
[2]Biomedical Engineering Group, Faculty of Electrical Engineering, Shahed University, Hasan Abad-e-Baqerof, Tehran, Tehran Province, Iran
[3]Department of Occupational Medicine, Faculty of Medicine, Tehran University of Medical Sciences, Tehran, District 6, Tehran Province, Iran
[4] Department of Cybernetics and Biomedical Engineering, Faculty of Electrical Engineering and Computer Science, VSB–Technical University of Ostrava, 17. listopadu 15, 708 33 Ostrava, Czech Republic
[5]Department of Electrical and Computer Engineering, College of Engineering, University of Texas El Paso, 500 W University Ave, El Paso, TX 79968, United States of America

amin.hekmatmanesh@lut.fi, mikaeili@shahed.ac.ir, sadeghniiat@tums.ac.ir, huapeng.wu@lut.fi, heikki.handroos@lut.fi, radek.martinek@vsb.cz, hnazeran@utep.edu

DOI: 10.15598/aeee.v15i3.2174

***Abstract.*** *It is well established that sleep spindles (bursts of oscillatory brain electrical activity) are significant indicators of learning, memory and some disease states. Therefore, many attempts have been made to detect these hallmark patterns automatically. In this pilot investigation, we paid special attention to nonlinear chaotic features of EEG signals (in combination with linear features) to investigate the detection and prediction of sleep spindles. These nonlinear features included: Higuchi's, Katz's and Sevcik's Fractal Dimensions, as well as the Largest Lyapunov Exponent and Kolmogorov's Entropy. It was shown that the intensity map of various nonlinear features derived from the constructive interference of spindle signals could improve the detection of the sleep spindles. It was also observed that the prediction of sleep spindles could be facilitated by means of the analysis of these maps. Two well-known classifiers, namely the Multi-Layer Perceptron (MLP) and the K-Nearest Neighbor (KNN) were used to distinguish between spindle and non-spindle patterns. The MLP classifier produced a high discriminative capacity (accuracy =* 94.93 *%, sensitivity =* 94.31 *% and specificity =* 95.28 *%) with significant robustness (accuracy ranging from* 91.33 *% to* 94.93 *%, sensitivity varying from* 91.20 *% to* 94.31 *%, and specificity extending from* 89.79 *% to* 95.28 *%) in separating spindles from non-spindles. This classifier also generated the best results in predicting sleep spindles based on chaotic features. In addition, the MLP was used to find out the best time window for predicting the sleep spindles, with the experimental results reaching* 97.96 *% accuracy.*

## Keywords

***Chaotic features, discriminative capacity, fractal dimension, intensity map, sleep EEG, spindle.***

## 1. Introduction

Spindles are part of the EEG signals recorded during sleep, which originate in the underlying physiological processes in the reticular nodules of the thalamus and extend to the cortex [1]. These bursts of oscillatory brain electrical activity are significant indicators of learning, memory and some disease states. Sleep is divided into Non-Rapid Eye Movement (NREM) and Rapid Eye movement that NREM contains three stages according to American Academy of Sleep Medicine (AASM) standard [1]. Sleep spindles, a hallmark pattern of sleep Stage 2, occur due to hippocampal ripples and are characterized by waveforms 0.5–2 seconds long with a frequency content of 12–14 Hz [2], [3] and [4]. Many studies have shown that there is a significant increase in the occurrence of sleep spindles with memory consolidation and encoding. In other words, more spindles are indicative of higher encoding and better recall [4], [5], [6], [7], [8] and [9]. Moreover, some diseases such as Alzheimer's [10], Rett Syndrome [11] and schizophrenia [12] may be potentially recognized based on the reliable and accurate detection of the number of spindles and their morphological properties. As manual scoring of sleep spindles is tedious and time consuming, researchers are eager to develop, test and validate computer-based algorithms to detect the occurrence of sleep spindles with a high discriminative capacity comparable to outcomes achievable by means of manual scoring.

To detect sleep spindles numerous methods have been developed to produce clinically acceptable results. A major part of the attempts has been focused on feature extraction. Huuppone et al. quantified the depth of sleep by using an amplitude feature as well as an innovative feature called the sigma index and detected sleep spindles derived from lateral channels with 70 % accuracy and 98.6 % sensitivity [13]. Typically, time series features are extracted from spindle shape. Rechtschaffen et al. used an amplitude threshold for spindle detection and reached 70 % accuracy [14]. Caldas da Costa et al. detected spindles by using their amplitude, morphological properties and statistical measures. They achieved a maximum accuracy of 96.6 % [15]. In contrast to time series, it has been shown that frequency or time-frequency features could produce better results. Ahmed et al. used wavelet packets to detect spindles and reached 93.7 % accuracy [16]. In another study, Duman et al. used Discrete Wavelet Transform (DWT) to detect spindles and achieved 92 % accuracy [17]. Najafi et al. used the Bump model, which is based on continuous Morlet wavelets, to detect spindles and reached 87.72 % accuracy with 99.49 % sensitivity [18]. Some researchers, including Duman et al., believe that the combination of different features could be useful. These authors performed sleep spindle detection with a sensitivity of 97.17 % by using three methods: Short-Time Fourier Transform (STFT); A Multiple Signal Classification Algorithm; and The Teager Energy Operator based on a decision tree [19]. Huupponen et al. used some specific methods such as phase-locked loop and complex demodulation, which resulted in 70 % accuracy with 97.7 % sensitivity [13]. Babadi et al. used a novel algorithm based on the Bayes method called DiBa, which separated spindles from non-spindle patterns and reached 96 % sensitivity [20]. Barros et al. detected sleep spindles by using the Independent Component Analysis (ICA) method [21].

Recently, many advanced approaches have been developed to interpret and quantify the behavior of nonlinear dynamical or chaotic systems [23] and [24]. These systems are capable of exhibiting a high level of fluctuations. The brain is an example of a chaotic system and the EEG signals generated by this organ reflect the summated fluctuations of excitatory and inhibitory postsynaptic potentials in the pyramidal cells of the upper layers of the cerebral cortex. As the underlying physiological system generating EEG signals is nonlinear, it is reasonable to expect that some specific nonlinear features extracted from these signals could be used to characterize and quantify the properties of transient waveforms that occur in them. For instance, Higuchi's, Katz's and Sevcik's Fractal Dimensions as well as LLE and Entropy measures may provide valuable information to detect and predict spindles as a short transient pattern. For instance, Acharya et al. used Katz's Fractal Dimension for sleep staging [22]. Allahverdy et al. used fractal dimension of EEG signals to diagnose Attention Deficit Hyperactivity Disorder (ADHD) in children [23]. Polychronaki et al. reported that fractal dimensions produced better results in epilepsy detection than other features [24].

Based on the advancements mentioned above and to improve automatic sleep spindle detection outcomes we utilized a variety of discriminative linear and nonlinear features and a mixture of them. In addition to time series features such as minimum, maximum, standard deviation, signal power, zero crossing and slope changes, we made use of four chaotic (nonlinear) features including the: Higuchi's Fractal Dimension (HFD); Katz's Fractal Dimension (KFD); Sevcik's Fractal Dimension (SFD); the Largest Lyapunov Exponent (LLE) and Kolmogorov's Entropy (KE).

Our investigation showed that chaotic features could give rise to adequate scattering in the feature space to produce significant accuracy (94.93 %) with notable robustness (3.6 % standard deviation) when a MLP classifier was used for spindle detection. In addition, in the detection part, we attempted to achieve the most similarity between spindle and non-spindle segments by choosing the non-spindle segments exactly one second before spindle occurrence. In order to provide a better sense of the adequacy of scattering in automatic spindle detection, we generated intensity map plots, spindle densities and spindle scattering. We also used chaotic features in spindle prediction. Experimentally, we showed that the chaotic features used for spindle detection improved the scattering. We arrived at the conclusion that: in order to achieve a better prediction, non-spindle features should be extracted from EEG segments approximately seven seconds before the occurrence of individual spindles.

$$z_m^k = \left\{z(m), z(m+k), z(m+2k), \ldots, z\left(m + \mathrm{int}\left(\frac{N-m}{k}\right)k\right)\right\}. \quad m = 1, 2, \ldots, k. \tag{1}$$

$$L_m(k) = \frac{\left\{\sum_{i=1}^{\mathrm{int}\left(\frac{N-m}{k}\right)}\right\} |z(m+ik) - z(m+(i-1)k)| \frac{(N-1)}{\mathrm{int}\left(\frac{N-m}{k}\right)k}}{k}. \tag{2}$$

## 2. Methods

To achieve improved spindle detection, both linear and nonlinear features were extracted from EEG signals. Various types of linear features (also called Time Series features) were used to detect sleep spindles. In this investigation, we used the same properties of the EEG signals that a specialist analyzes to distinguish between sleep spindles from non-spindles. These features mainly included Zero Crossing (ZCR) and maximum (Max) amplitude in 0.5–2 s time windows. Moreover, inspired by a number of previous studies we also made use of other linear features such as mean amplitude (Mean), minimum amplitude (Min), Standard Deviation (SD) and power spectral density (PSD) calculated over 0.5–2 s time windows [15] and [16].

In addition to the linear features describe above, we used a variety of nonlinear features as described in the sections below.

### 2.1. Higuchi's Fractal Dimension (HFD)

The fractal dimension of the basin of attraction is one of the measures used to recognize dynamic behavior limitations and show the degrees of freedom of a time series. The HFD is a measure based on different signal lengths and their prediction with different time delays. For a time series, the k time series construction is defined as Eq. (1), [25], where $m$ is the initial point, $k$ is the reconstruction delay and $\mathrm{int}(x)$ is used to calculate the integer part of $x$. The length of the new time series $L_m(k)$ is defined as Eq. (2), where $(N-1)/(\mathrm{int}((N-m)/k)\cdot k)$ is the normalization factor. The average length of the time series is measured by averaging $L_m(k)$, that is $L(k) = \frac{1}{k}\sum_{m=1}^{k} L_m(k)$. Here is proportional to $k^{FD}$, where $FD$ is the fractal dimension value. In this study the Higuchi fractal dimension was calculated from: $\log(L(k))$ versus $\log(1/k)$ graph.

### 2.2. Katz's Fractal Dimension (KFD)

In 1988, Katz proposed a new method to estimate the fractal dimension [26]. In this method the distance between the real data points was used to create a curve comprised of the minimum number of points necessary to do so. This fractal dimension was calculated as Eq. (3), [26] and [27], where $N$ is the total number of data points, $L$ is the total length of the reconstructed path and $d$ is the diameter or planar extent of the waveform.

$$FD = \frac{\log(N-1)}{\log(N-1) + \log\left(\frac{d}{L}\right)}. \tag{3}$$

### 2.3. Sevcik's Fractal Dimension (SFD)

Sevcik showed that fractal dimension could be approximated by $N$ signal samples. The Sevcik's Method is based on the normalization of EEG signals and time axes [28] and [29]. The SFD is formulated as Eq. (4), where $L$ is the total length of the normalized signal and $N$ is the total number of points to be calculated.

$$FD = 1 + \frac{\ln(L)}{\ln(2(N-1))}. \tag{4}$$

### 2.4. Largest Lyapunov Exponent (LLE)

The LLE Method was proposed by Wolf in 1985 [23] to compute how fast a nonlinear dynamic system reaches chaotic behavior. The basic concept underlying the LLE Method is that after reconstructing the phase space, the nearest neighbor is sought to find the initial embedding vector with the following criterion [23]. Neighbors should be separated in time to prevent consecutive vectors of nearest neighbor to fall in the same trajectories [23]. While trajectories are growing, distance between two trajectories are computed with a pre-determined delay which is calculated by using the Minimum of value of the Mutual Information (MMI) [30] and [31], which means minimum dependency between two trajectories [30]. The LLE is based on Eq. (5) as follows, [23] and [30], where $k$ is the number of steps in which distances will be measured. $L(t_i)$ and $L(t_{i-1})$ are the distances between the nearest pair of state vectors at time ti and the next time step, respectively.

$$L_1 = \frac{1}{t_k - t_0} \sum_{i}^{k} \ln \frac{L'(t_i)}{L(t_{i-1})}. \quad (5)$$

## 2.5. Kolmogorov's Entropy (KE)

The Kolmogorov's Entropy (KE) is another parameter used to quantify chaotic behavior, which is also based on the phase space concept. The phase space is a space, which represents all of the possible states of a system with each point uniquely representing each one of those states. It is a multi-dimensional space whose degrees of freedom represent the number of axes in the multi-dimensional space [31]. In this method, the phase space is segmented into cells (multi-dimensional hyper-cubes) and the probability that the trajectories are in these hypercubes is used to calculate KE shown as $S_n$ below. This quantifier is also interpreted as the level of a system's complexity and its tendency to behave chaotically. Complexity is calculated based on the regularity of trajectories. An increase in trajectory regularity is indicative of a decrease in complexity and vice versa. $S_n$ is calculated as Eq. (6), [31], where $q(i)$ is the probability of the occurrence of the trajectories in the phase space cells.

$$S_n = -\sum_{i} q(i) \cdot \ln q(i). \quad (6)$$

## 2.6. Data Analysis - Statistical Measures

We interpreted our results based on three statistical parameters (as defined by the formulas below and collectively called the discriminative capacity) for our purposes here. A True Positive (TP) result is achieved when a detected spindle by the algorithm agrees with that of the expert. A True Negative (TN) result is obtained if the absence of a spindle is correctly detected. A False Positive (FP) result is set when the automatic algorithm detects the presence of a spindle and there is no spindle detected in manual scoring. On the contrary, a False Negative (FN) result is set when the algorithm does not detect a spindle while the expert scores its occurrence [15]:

$$\text{Sensitivity} = \text{SEN} = \frac{\text{TP}}{\text{TP} + \text{FN}}, \quad (7)$$

$$\text{Specificity} = \text{SPE} = \frac{\text{TN}}{\text{FP} + \text{TN}}, \quad (8)$$

$$\text{Accuracy} = \text{ACC} = \frac{\text{TP} + \text{TN}}{\text{TP} + \text{TN} + \text{FP} + \text{FN}}. \quad (9)$$

## 2.7. Data Acquisition

The data were recorded using an EMBLA System (Version N7000, Natus Medical, USA) with 10 channels including: C3-M2, C4-M1, Cz-M1, F4-M1, F3-M2, Fz-M1, T3-M2, T4-M1, O2-M1, and O1-M2. All channels were recorded with reference to both mastoids based on the 10–20 International Electrode Placement System, where M1 and M2 are the left and right Mastoids, respectively. The sleep EEG data acquired from C3-M2 and C4-M1 channels were used to extract spindle features. Sleep stages were scored according to the American Academy of Sleep Medicine (AASM) Standard. Our specialist at the Baharloo Sleep Research Center scored 720 spindles in sleep Stage 2 from C3-M2 and C4-M1 channels. The aggregate spindle lengths were 885.4 seconds, with 0.5 sec as the shortest and 1.8 seconds as the longest length. The sampling frequency was set to 200 Hz and the electrode contact impedance was maintained below 5 kΩ.

In order to find the best time window position for spindle prediction, a one second non-overlapping sliding window was selected as the non-spindle segment. Based on our experience, the maximum time between every two spindles are usually 10 seconds or more. So, we started the sliding window from 10 seconds before any spindle to avoid taking a segment with spindle as a non-spindle one. For each window position, non-spindle features were extracted and classified. The best result among the 10 segment positions was in the seventh second window before spindle occurrence with a 97.96 % accuracy. Also, by considering the average TP and TN results, the best result corresponded with the 7$^{\text{th}}$ second before spindles. The results are the average of 9 repeats of training and testing.

# 3. Experimental Setup

## 3.1. Subjects

Twenty-two healthy subjects (11 males, 11 females with an average age of 22.3 years, and a range of 22–26 years) participated in this study. However, complete and quality assured data from only ten subjects (5 males and 5 females) could be used for this investigation as two subjects did not follow proper instructions. Ethics approval was obtained from the Medical Research Ethics Committee (MREC) of Shahed University. All subjects signed an informed letter of consent before participation in the study. EEG signals were acquired from these participants in the Baharloo Sleep Research Center (Tehran, Iran) by using the International 10-20 EEG Electrode Placement System. Subjects were advised not to use any products containing nicotine and/or caffeine for at least four hours before their participation in the test. Subjects slept for two sequential days in the afternoons for approximately one and half hours: the first day was for the subjects to adapt to the environment and provide baseline data and the second was the main day for data acquisition (subjects experienced specific emotional stimuli by watching a variety of pictures selected from the International Affective Picture System - IAPS – before preparing to go to sleep).

### 3.2. Signal Processing

Using the EMBLA System's software, EEG signals were first filtered with a 50 Hz notch filter to remove power-line noise. A 0.3 Hz high-pass and then a 40 Hz low-pass filter were used to pass frequencies between 0.3–40 Hz. Subsequently, filtered signals were further processed using a $16^{\text{th}}$ order IIR type-II Chebyshev band-pass filter with corner frequencies of 8 and 16 Hz based on spindle frequency definitions (the type and order of the filter were selected experimentally), [16]. Performing zero-phase digital filtering eliminated the large amount of phase distortion generated by this filter. This was achieved by means of feeding the input signal to the filter once in the forward and once in the reverse direction [32]. A total of 720 spindle and 720 non-spindle signals were processed. Features were divided into two categories:

- time series features, which are based on those properties of the spindles that an expert would use to detect them visually,
- nonlinear features, which are measures that are not visually detectable by the expert.

Due to the non-stationary character of EEG signals, they were first segmented using one-second windows [16] and [17]. With this approach, it was possible to assume signal stationarity [17]. The one-second time windows were positioned at the beginning of the spindles even though their lengths could have been more than or less than one second. The non-spindle signals for training the classifier were chosen exactly one second right before the occurrence of spindles. One reason for selecting the non-spindle signals as mentioned above was to make sure that they occurred in sleep Stage 2, the second reason was to ensure the existence of the most similarity between two signal segments, and the third reason was to assure that the non-spindle segments would not contain spindles. To validate the segmentation process, all segments were checked manually. Consequently, we were able to show the utility of these chaotic features in the classification of data in the feature space.

The extracted features were automatically discerned by using the $K^{\text{th}}$ Nearest Neighbor (KNN) and Multi-Layer Perceptron (MLP) classifiers. To classify the scored (720) spindles, the dataset were folded into nine folds such that each fold contained 80 spindles. One fold was selected randomly as the test dataset while the other folds were chosen as the training dataset. The reported results are the average of nine repeats of training and testing. The MLP classifier properties were as follows: 7 neurons were contained in the hidden layer with "Logsig" as the transfer function, six data points from each fold of training data were withdrawn for random cross-validation, and the output function was a linear neuron. In order to use the KNN classifier, different distance measures were used to choose the nearest neighbor to classify, with the best distance being one. To find the best time location for predicting the spindle pattern the same classification procedure was used. The one-second non-spindle segments were moved from 1 to 10 seconds before the occurrence of each spindle segment.

## 4. Results

It is well established that the probability of spindle detection increases with an increase in the intensity of scattering between features [33] and wider scattering can produce good decision boundary in categorizing data. Figure 2 shows a comparison between the scattering of chaotic (nonlinear) and linear features. It is clear that the chaotic features produce a wider scattering than linear features. It is also evident that the linear features have more overlap compared to the chaotic features.

The intensity maps showing the degree of scattering of different nonlinear feature pairs are shown in Fig. 3, Fig. 4, Fig. 5, Fig. 6 and Fig. 7. In these 3-D figures, the vertical axes represent the scattering ratios (densities or intensities). The color range in the intensity maps indicate the level of scattering. A brighter color means a higher scattering, which indicates a higher probability of spindle detection and vice versa.

Figure 3 shows the degree of scattering of Higuchi's and Sevcik's features. This figure demonstrates that the density of spindles varies over a wide range and the probability of spindle detection would increase if feature scattering was enhanced.

It is observed that different FD features have scattering measures that could be used effectively to detect sleep spindles. The bright colors in Fig. 3 show that the intensity map of Higuchi's and Sevcik's features are interestingly independent and that the scattering is more separated (Please compare to Fig. 4, Fig. 5, Fig. 6 and Fig. 7 below and see Tab. 3).

In this section we first reflect on the results that show how the degree of scattering of linear and non-

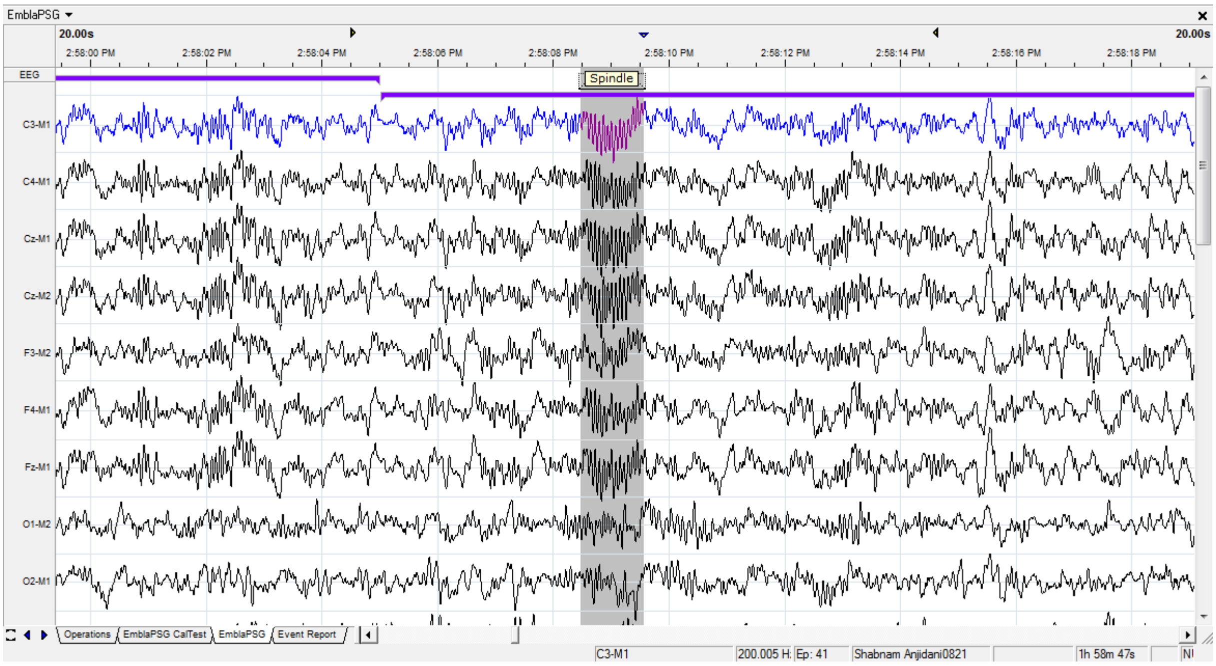


**Fig. 1:** An example of a detected Spindle in sleep Stage 2.

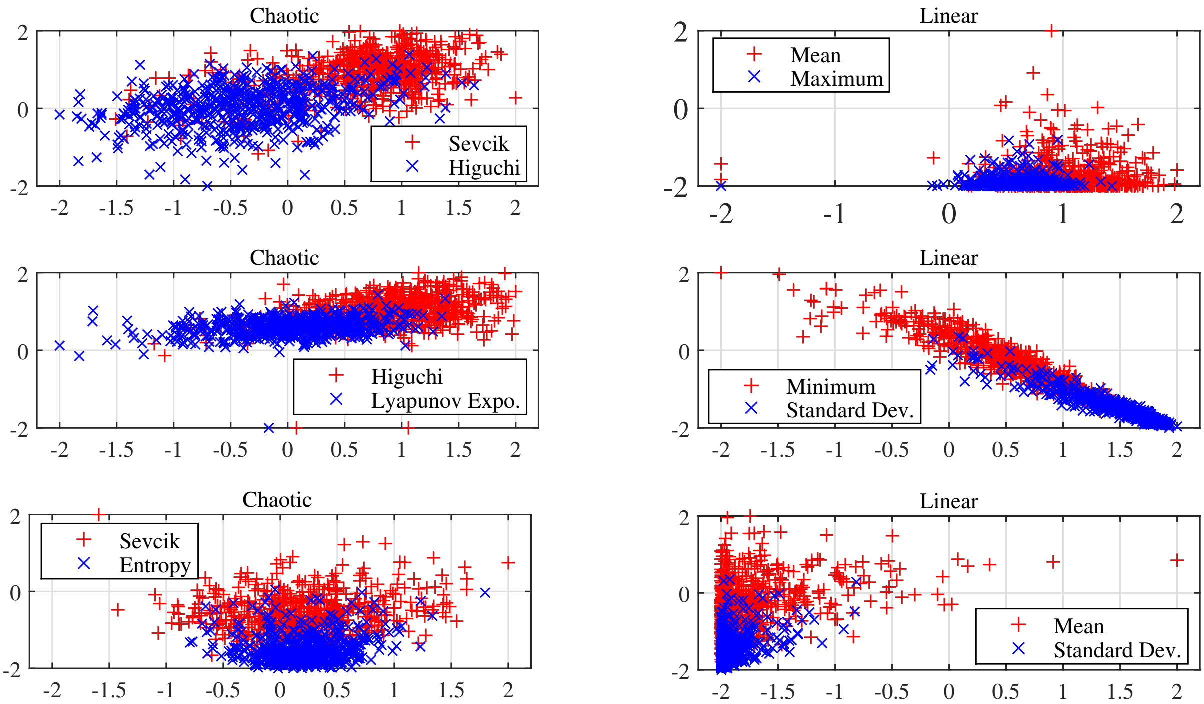


**Fig. 2:** A comparison between the scattering of chaotic (nonlinear) and linear features. It is clear that the chaotic features produce a wider scattering than linear features. It is also evident that the linear features have more overlap compared to the chaotic features. Wider scattering can produce good decision boundary in categorizing data.

**Tab. 1:** Discriminative capacity (accuracy, sensitivity and specificity) produced by the MLP classifier using different features.

| Neural Network (MLP) | Accuracy (%) | Sensitivity (%) | Specificity (%) |
|---|---|---|---|
| Time-series features | 92.15±5.8 | 91.25±1.5 | 93.06±8.0 |
| Chaotic features | 93.24±3.00 | 92.15±0.2 | 94.31±2.9 |
| Time-series and Chaotic features | 94.93±1.89 | 94.58±0.16 | 95.28±0.8 |

**Tab. 2:** Discriminative capacity (accuracy, sensitivity and specificity) produced by the KNN classifier.

| K-Nearest Neighbor | Accuracy (%) | Sensitivity (%) | Specificity (%) |
|---|---|---|---|
| Time-series features | 87.98 | 88.00 | 87.96 |
| Chaotic features | 86.32 | 89.91 | 82.73 |
| Time-series and Chaotic features | 83.75 | 85.36 | 82.14 |

**Tab. 3:** The scattering of different features expressed in terms of Standard Deviation (SD), chaotic and some of the linear features. ZCR is the abbreviation of Zero Crossing feature of waveforms. LLE is Largest Lyapunov Exponent.

| Spindle | KFD | SFD | HFD | LLE | Entropy | Mean | Max | Min | SD | ZCR | ZCR Density |
|---|---|---|---|---|---|---|---|---|---|---|---|
| SD | 8.524 | 10.741 | 11.942 | 1.2007 | 11.529 | 9.525 | 8.123 | 8.127 | 8.3714 | 10.03 | 10.55 |
| Min | 0.1248 | 1.3413 | 0 | 1.2278 | $-6.68 \cdot 10^{-7}$ | $6.06 \cdot 10^{-6}$ | $-5.5 \cdot 10^{-5}$ | $2.82 \cdot 10^{-6}$ | 2.06 | 18 | 20 |
| Max | 0.291 | 1.512 | 1.024 | 1.0819 | $5.50 \cdot 10^{-7}$ | $5.83 \cdot 10^{-5}$ | $-6.4 \cdot 10^{-6}$ | $2.14 \cdot 10^{-5}$ | 2.620 | 31 | 31 |
| Mean | 0.2294 | 1.4548 | 0.7603 | 7.9379 | $2.21 \cdot 10^{-9}$ | $2.36 \cdot 10^{-5}$ | $-2.3 \cdot 10^{-5}$ | $1.06 \cdot 10^{-5}$ | 2.484 | 26.44 | 26.894 |

linear features as well as the intensity maps of various nonlinear features derived from the constructive interference of spindle signals could improve the detection of the sleep spindles and how the prediction of sleep spindles could be facilitated by means of the analysis of these maps (To gain an appreciation for the wave shape of sleep spindles, Fig. 1 shows an example). We then present the results of our pilot investigation based on automatic classification outcomes achieved by using 3 types of features (time series, chaotic measures, and a mixture of them) and 2 classifiers (KNN and MLP). We show that nonlinear neurons in the MLP and the chaotic features improved the detection and prediction outcomes.

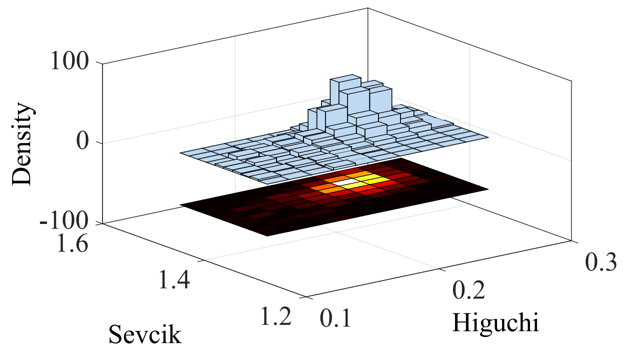


**Fig. 3:** Intensity scattering distribution map of Higuchi's and Sevcik's FDs. This map indicates that the intensity scattering map of these features could be applied effectively for detection of sleep spindles.

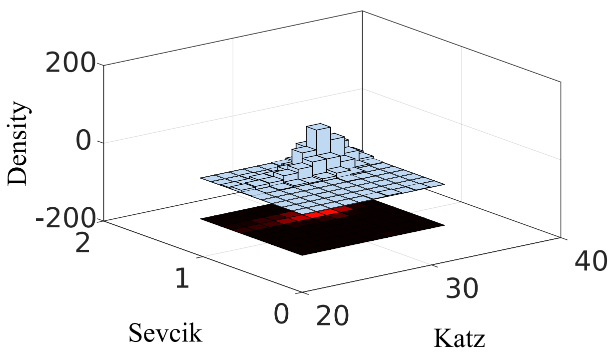


**Fig. 4:** Intensity map distribution of the Sevcik versus Katz fractal dimension. The dark colors in the intensity scattering map indicate the low dependency of Sevcik's and Katz's FDs in the feature space. Thus, the map indicates low scattering of Katz's fractal dimension that has destructive interaction against Sevcik's FD.

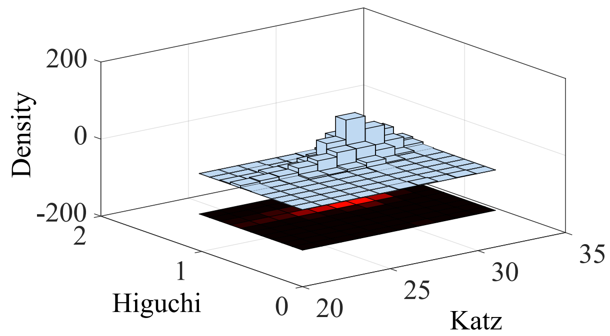


**Fig. 5:** Intensity map distribution of the HFD versus KFD. This map indicates the low scattering and destructive interaction role of Katz's FD against Higuchi's. The low scattering leads to the low dependence of spindle detection on Higuchi's and Katz's features.

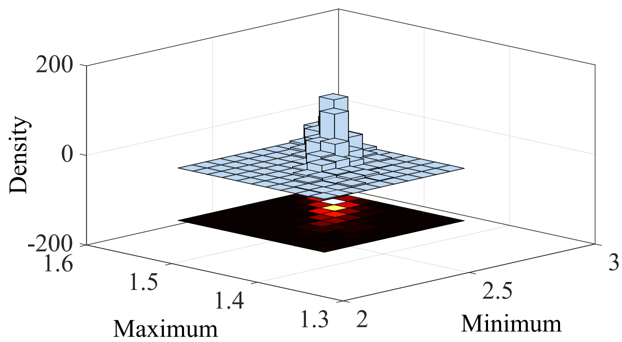


**Fig. 6:** Intensity map distribution of the Maximum versus the Minimum features. This map demonstrates the dependence of spindle detection on Minimum and Maximum linear features.

**Tab. 4:** Spindle prediction (Experimental results).

| Non-spindle lead time window (sec) before spindle occurrence | Experimental prediction results maximum accuracy (%) | Average TP results across folds | Average TN results across folds |
|---|---|---|---|
| 2 | $75.69 \pm 5.3$ | $74.00 \pm 1$ | $74.00 \pm 5$ |
| 3 | $78.81 \pm 6.0$ | $69.25 \pm 1$ | $74.00 \pm 5$ |
| 4 | $75.47 \pm 3.3$ | $72.62 \pm 1$ | $71.00 \pm 5$ |
| 5 | $70.97 \pm 2.9$ | $71.50 \pm 1$ | $72.87 \pm 5$ |
| 6 | $83.76 \pm 3.0$ | $72.50 \pm 0$ | $73.12 \pm 4$ |
| **7** | **$97.96 \pm 2.4$** | **$81.12 \pm 0$** | **$79.60 \pm 3$** |
| 8 | $92.07 \pm 4.3$ | $74.12 \pm 1$ | $71.87 \pm 3$ |
| 9 | $91.81 \pm 5.8$ | $71.62 \pm 1$ | $73.5 \pm 4$ |
| 10 | $89.58 \pm 4.1$ | $72.50 \pm 0$ | $72.87 \pm 4$ |

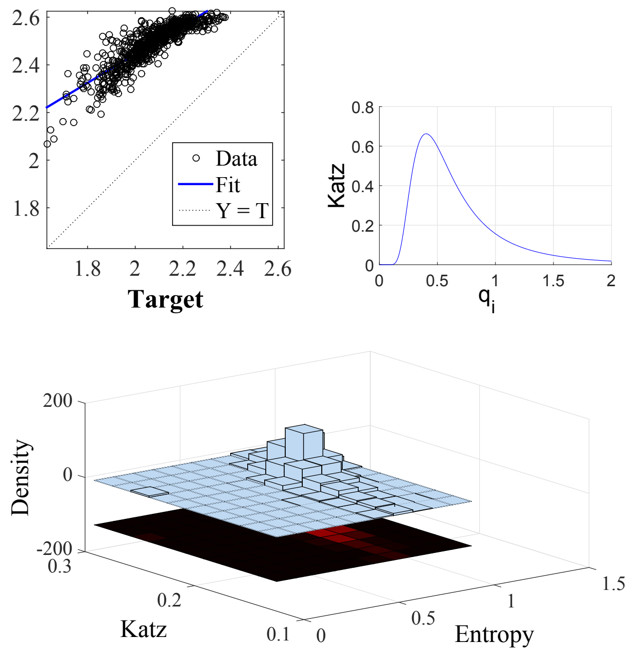


**Fig. 7:** Intensity map distribution of KFD versus Entropy. The scattering in the figure emerges from the dependence of the Katz's fractal dimension on the parameter ($q$) in the experimental results and the curve shown on the upper right of the figure reflects the dependence of the KFD on the parameter ($q$) in the production of the theoretical results.

Figure 4 and Fig. 5 reveal that Katz's model shows a low scattering measure compared to other chaotic features. The high intensity map with high scattering measure in Higuchi's features and Sevcik's features makes these features suitable for spindle detection. The effectiveness of this point is shown in Fig. 3. Simultaneously the large scattering and independency in the intensity map could explain the detection of spindles in another method (Fig. 6).

Figure 7 displays the intensity map of the KFD as a function of Entropy. It is shown that the scattering of EEG signals for this feature is improved by the use of Entropy properties. The scattering of EEG signals could be explained by means of the numbers of occurrences in the trajectory over the given time interval. It is well known that the intensity map distribution depends on the number of occurrences in a considered cell. Also it should be mentioned that, the scattering of the intensity map in the Katz model depends mainly on the ($g$) parameter. Since $q(i)$ is taken into account in an arbitrary time interval window, the KFD could be applied to the intensity map to consider its scattering versus Entropy with both of them being time dependent. As a result one can demonstrate that scattering of these features can be meaningful and could serve as a distinguishing feature in the time domain.

A chaotic feature, which is commonly used in weather prediction and is also useful in biosignal processing, is the LLE. This feature indicates how fast the system moves towards chaos and a higher value means a higher speed and vice versa. The average value for non-spindle LLE feature was 2.5246 and for spindle feature was 7.9379, respectively. This shows that when the brain produces spindles, on average it's behavior changes toward chaos for a period of about 2 seconds and then changes to the previous state. Also, the difference between these two average values in comparison with other features is appropriate for an algorithm to make the decision. Based upon the SD, Minimum and Maximum values in Tab. 3, and the scattering and intensity map in Fig. 8 it can be expected that the LLE

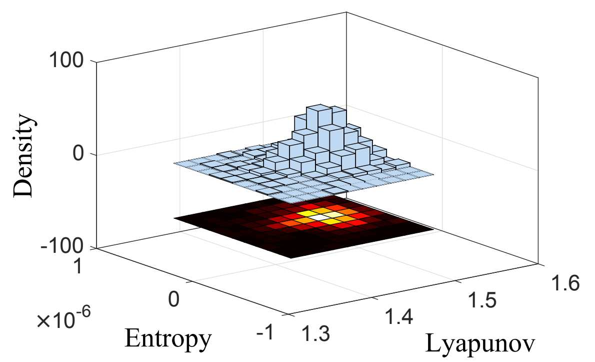


**Fig. 8:** Intensity map of the Entropy versus LLE. The scattering shows the highest independency in comparison to the other features.

may have the best efficacy in comparison to other features.

Table 1, Tab. 2 and Tab. 4 summarize the results. The spindle detection results by means of the MLP classifier using time series (as linear) features; chaotic (as nonlinear) features and their combination are shown in Tab. 1. It is clear that with the MLP as the classifier with the mixture of linear and nonlinear features produced a noticeable effect in the detection outcomes in comparison to the results when time series or chaotic features were used alone (Tab. 1). The comparison results for the KNN classifier based on the three different types of features mentioned above are presented in Tab. 2. The average quantified feature values of the spindles with four parameters that included Standard Deviation, Minimum, Maximum and Average are shown in Tab. 3. One-second segments (time windows) were used to extract spindle and non-spindle properties before spindle occurrence. The spindle prediction outcomes based on using 10 different lead time windows (starting 1 second to 10 seconds before spindle occurrence) for non-spindle segments are presented in Tab. 4. This table shows that starting the non-spindle signal processing window 7 seconds before the occurrence of sleep spindles produced the best spindle prediction accuracy at 97.96 %. Please note that Tab. 4 shows the results of spindle prediction by using the MLP classifier.

## 5. Discussion

As it is evident from the results, the quality of detection and prediction of spindles are highly dependent on both linear and nonlinear features. In the sleep literature, it is well established that there are a variety of linear features that could be used for spindle detection. In this investigation our sleep specialist used some linear features (such as Mean, Max, Min, SD, and ZCR, collectively listed as time-series features) to characterize sleep spindles by their morphology. From Tab. 1, one can observe the impact of linear and nonlinear features on producing improved classification outcomes. In our study, in addition to using linear features we considered the use of nonlinear features to achieve better detection and prediction, and utilized two classifiers such as MLP and KNN to automatically classify sleep spindles. The linear features could produce a maximum accuracy of 92.15 %. The detection accuracy was further improved by inclusion of some nonlinear features. In other words, it was shown that proper selection of nonlinear features and their addition to the feature vector fed to the classifiers could result in an improvement in spindle detection accuracy of these algorithms. This improvement could be attributed to the nonlinear properties of EEG signals. In fact, nonlinear features could carry information on some attributes of the EEG signals, which are not visually evident.

The chaotic features that we selected as specific nonlinear features could improve the detection outcomes due to the fact that they produced wider scattering and less overlap in the feature space (Fig. 1 and Tab. 3); this in turn could provide a better decision boundary for automatic classification. As can be seen in Tab. 1 and Tab. 2, wider scattering of features increased the classification accuracy to 93.24 %. Furthermore, it was possible to achieve improved detection outcomes by mixing time series and chaotic features. The incremental improvement achieved in this case could be attributable to the complexity and nonlinear properties of the EEG signals captured by these nonlinear features. In addition, our results showed that leveraging the discriminative powers of both linear and nonlinear features enabled us to achieve not only better accuracy (94.93 %) but also higher efficiency. As a consequence of these advantages, we decided to adopt the same approach in our sleep spindle prediction research. In this investigation we also observed that the Fractal dimensions (FDs), the Largest Lyapunov Exponent (LLE) and Kolmogorov's Entropy of EEG signals, as a set of chaotic features, neatly fulfilled our objective in detecting sleep spindles. The FD features measure self-similarity in EEG signals effectively. One of the best ways to show the self-similarity that occurs in EEG signals was to use Katz's, Higuchi's and Sevcik's Fractal Dimensions. The scattering of these nonlinear features is shown in Fig. 2. It is observed that notable scattering of FDs is a critical attribute of these features in producing excellent results in the detection of spindles and non-spindles. However, it is remarkable to note that the Katz's model of FD features produced inferior results in spindle detection. This could be explained by focusing on the Katz's formula. According to this formula [27], it was expected that the maximum diagonal distance between samples would occur between the first and the end sample ($d$ point is the maximum diameter or planar extent of the waveform). But the spindles' shape created a distortion in the maximum distance, which was found around the middle of the spindles in our study.

As reported in Tab. 3, the SD and the differences between Maximum and Minimum values in the KFD are less than other features. The weakness of KFD in spindle detection and the intensity map with low scattering are revealed, which could effectively explain the noticeable spindle detection of other FD features except Katz's in a similar manner.

We also observed that the nonlinear properties of the MLP classifier resulted in more accurate detection of sleep spindles in comparison to the KNN classifier. This improvement was due to the inclusion of nonlinear functions of the MLP classifiers acting as neurons to deal with an enormous range of data. On the other hand, in the KNN classifiers the curse of dimensionality occurs for the huge data range. The MLP classifiers are suitable for use with chaotic features and the best explanation for the excellent results shown in Tab. 1 is that we used different nonlinear chaotic features to achieve these outcomes. Since nonlinear features are applied to represent EEG signals, a set of these features may capture the nonlinear properties of the EEG signals more accurately.

Overall, our pilot investigation revealed that the efficacy of sleep spindle detection could be explained by means of scattering and intensity map distribution of nonlinear FD features. By thorough exploration, one can find that the KFD is rather weak compared to the other FDs. Simultaneously; the high coherence of the scattering map in the Sevcik and Higuchi features could effectively be applied in spindle detection. The difference between Minimum and Maximum values, which are experimental to obtain, is measureable by a parallel method that could be used for spindle detection (Tab. 3).

Here we summarize the detection and prediction of spindles by making use of intensity map diagram as an effective tool. The "Density" in the intensity map diagram increases slightly or even considerably as a function of the scattering in the nonlinear features of spindles. Initially, there is no spindle wave in the processing window. As time increases, the window slides over the signal until a spindle wave enters the window. Up to this point the intensity has its minimal value (non-spindle segments). As the spindle waves enter the window, the "Density" in the intensity map keeps growing until the whole spindle set is inside the window. This process could be best explained, by means of perturbations in the scattering map of nonlinear chaotic features. These perturbations lead to an increase in amplification of the intensity, which results in a constructive interference of maxima in the map. The sum over all possible maxima in the intensity map would result in maximum intensity in the nonlinear features, which is in complete agreement with the maximum distribution function. This explanation is in good agreement with the previous consideration about the scattering of nonlinear chaotic features (Fig. 2). Using this explanation, one can predict sleep spindles in the EEG spectrum by means of the intensity map distribution function. In our experiments we found that the average prediction robustness could achieve a standard deviation of 3.6 % after 9 times training with the MLP classifier.

# 6. Conclusion

In this paper we discussed how we made use of a mixture of linear and nonlinear features as well as two classifiers to perform sleep spindle detection and prediction. We used two well-known classifiers, the KNN and MLP with the K-fold method and observed that the MLP classifier achieved the best results with higher robustness. Our results indicated that leveraging the combined power of chaotic and time series features enabled us to better characterize the properties of EEG signals for more accurate detection and of sleep spindles. Using the nonlinear properties of EEG signals, our experimental findings were further validated with our results by using intensity distribution maps. It was shown that the efficacy of sleep spindle detection and prediction could be best explained by using the intensity distribution function as an effective visualization tool. Also, we showed that the robustness of the detection accuracy improved notably after training the MLP classifier 9 times. In our future research in Finland, we intend to extend the utility of these methods to robotic therapy research with the objective to detect and predict the motor behavior of the human brain with a specific focus on stroke patients.

# References

[1] COTE, K. A., T. M. EPPS and K. B. CAMPBELL. The role of the spindle in human information processing of high-intensity stimuli during sleep. *Journal of sleep research*. 2000, vol. 9, no. 1, pp. 19–26. ISSN 1365-2869. DOI: 10.1046/j.1365-2869.2000.00188.x.

[2] SHELDON, S. H., M. H. KRYGER, R. FERBER and D. GOZAL. *Principles and Practice of Pediatric Sleep Medicine*. 2nd ed. London: Elsevier Health Sciences, 2014. ISBN 978-1-4557-0318-0.

[3] LOOMIS, A. L., E. N. HARVEY and G. HOBART. Potential rhythms of the cerebral cortex during sleep. *Science*. 1935, vol. 81, no. 2111, pp. 597–598. ISSN 1095-9203. DOI: 10.1126/science.81.2111.597.

[4] SIROTA, A., J. CSICSVARI, D. BUHL and G. BUZSAKI. Communication between neocortex and hippocampus during sleep in rodents. *Proceedings of the National Academy of Sciences*. 2003, vol. 100, no. 4, pp. 2065–2069. ISSN 1091-6490. DOI: 10.1073/pnas.0437938100.

[5] RUCH, S., O. MARKES, S. B. DUSS, D. OPPLIGER, T. P. REBER, T. KOENIG, J. MATHIS, C. ROTH and K. HENKE. Sleep stage II contributes to the consolidation of declarative memories. *Neuropsychologia*. 2012, vol. 50, no. 10, pp. 2389–2396. ISSN 1873-3514. DOI: j.neuropsychologia.2012.06.008.

[6] SCHABUS, M., G. GRUBER, S. PARAPATICS, C. SAUTER, G. KLOSCH, P. ANDERER, W. KLIMESCH, B. SALETU and J. ZEITLHOFER. Sleep Spindles and Their Significance for Declarative Memory Consolidation. *Sleep*. 2004, vol. 27, no. 8, pp. 1479–1485. ISSN 1550-9109. DOI: 10.1093/sleep/27.7.1479.

[7] ANDERER, P., G. GRUBER, G. KLOSCH, W. KLIMESCH, B. SALETU and J. ZEITLHOFER. Sleep and memory consolidation: The role of electrophysiological neuroimaging. *Somnologie*. 2002, vol. 6, no. 2, pp. 54–62. ISSN 1439-054X. DOI: 10.1046/j.1439-054X.2002.02175.x.

[8] ELLENBOGEN, J. M., J. D. PAYNE and R. STICKGOLD. The role of sleep in declarative memory consolidation: passive, permissive, active or none? *Current opinion in neurobiology*. 2006, vol. 16, no. 6, pp. 716–722. ISSN 0959-4388. DOI: 10.1016/j.conb.2006.10.006.

[9] CLEMENS, Z., D. FABO and P. HALASZ. Overnight verbal memory retention correlates with the number of sleep spindles. *Neuroscience*. 2005, vol. 132, no. 2, pp. 529–535. ISSN 0306-4522. DOI: 10.1016/j.neuroscience.2005.01.011.

[10] DAUWELS, J., F. VIALATTE and A. CICHOCKI. Diagnosis of Alzheimers Disease from EEG Signals: Where Are We Standing? *Current Alzheimer Research*. 2010, vol. 7, no. 6, pp. 487–505. ISSN 1875-5828. DOI: 10.2174/156720510792231720.

[11] GAROFALO, E. A., I. DRURY and G. W. GOLDSTEIN. EEG Abnormalities Aid Diagnosis of Rett Syndrome. *Pediatric neurology*. 1988, vol. 4, no. 6, pp. 350–353. ISSN 0887-8994.

[12] WAMSLEY, E. J., M. A. TUCKER, A. K. SHINN, K. E. ONO, S. K. MCKINLEY, A. V. ELY, D. C. GOFF, R. STICKGOLD and D. S. MANOACH. Reduced Sleep Spindles and Spindle Coherence in Schizophrenia: Mechanisms of Impaired Memory Consolidation? *Biological psychiatry*. 2012, vol. 71, no. 2, pp. 154–161. ISSN 1873-2402. DOI: 10.1016/j.biopsych.2011.08.008.

[13] HUUPPONEN, E., G. GOMEZ-HERRERO, A. SAASTAMOINEN, A. VARRI, J. HASAN and S.-L. HIMANEN. Development and comparison of four sleep spindle detection methods. *Artificial Intelligence in Medicine*. 2007, vol. 40, no. 3, pp. 157–170. ISSN 0933-3657. DOI: 10.1016/j.artmed.2007.04.003.

[14] RECHTSCHAFFEN, A. and A. KALES. A manual of standardized terminology, techniques and scoring system for sleep stages of human subjects. *Clinical Neurophysiology*. 1968, vol. 26, no. 6, pp. 644–701. ISSN 1388-2457. DOI: 10.1016/0013-4694(69)90021-2.

[15] DA COSTA, J. C., M. D. ORTIGUEIRA, A. BATISTA and T. SANTOS PAIVA. Threshold choice for automatic spindle detection. In: *19th International Conference on Systems, Signals and Image Processing*. Wien: IEEE, 2012, pp. 197–200. ISBN 978-3-200-02328-4.

[16] HEKMATMANESH, A., S. M. R. NOORI and M. MIKAILI. Sleep spindle detection using modified extreme learning machine generalized radial basis function method. In: *22nd Iranian Conference on Electrical Engineering*. Teheran: IEEE, 2014, pp. 1898–1902. ISBN 978-1-4799-4409-5. DOI: 10.1109/IranianCEE.2014.6999850.

[17] ACCARDO, A., M. AFFINITO, M. CARROZZI and M. BOUQUET. Use of the fractal dimension for the analysis of electroencephalographic time series. *Biological cybernetics*. 1997, vol. 77, no. 5, pp. 339–350. ISSN 0340-1200. DOI: 10.1007/s004220050394.

[18] NAJAFI, M., Z. GHANBARI, B. MOLAEE-ARDEKANI, M.-B. SHAMSOLLAHI and T. PENZEL. Sleep spindle detection in sleep EEG signal using sparse bump modeling. In: *1st Middle East Conference on Biomedical Engineering*. Sharjah: IEEE, 2011, pp. 196–199. ISBN 978-1-4244-7000-6. DOI: 10.1109/MECBME.2011.5752099.

[19] DUMAN, F., A. ERDAMAR, O. EROGUL, Z. TELATAR and S. YETKIN. Efficient sleep spindle detection algorithm with decision tree. *Expert Systems with Applications*. 2009, vol. 36, no. 6, pp. 9980–9985. ISSN 0957-4174. DOI: 10.1016/j.eswa.2009.01.061.

[20] BABADI, B., S. M. MCKINNEY, V. TAROKH and J. M. ELLENBOGEN. DiBa: A Data-Driven Bayesian Algorithm for Sleep Spindle Detection. *IEEE Transactions on Biomedical Engineering*. 2012, vol. 59, no. 2, pp. 483–493. ISSN 1558-2531. DOI: 10.1109/TBME.2011.2175225.

[21] BARROS, A. K., R. ROSIPAL, M. GIROLAMI, G. DORFFNER and N. OHNISHI. Extraction of Sleep-Spindles from the Electroencephalogram

(EEG). In: *Artificial Neural Networks in Medicine and Biology*. Goteborg: Springer, 2000, pp. 125–130. ISBN 978-1-4471-0513-8.

[22] ACHARYA, R. U., O. FAUST, N. KANNATHAL, T. CHUA and S. LAXMINARAYAN. Non-linear analysis of EEG signals at various sleep stages. *Computer Methods and Programs in Biomedicine*. 2005, vol. 80, no. 1, pp. 37–45. ISSN 0169-2607. DOI: 10.1016/j.cmpb.2005.06.011.

[23] ALLAHVERDY, A., A. M. NASRABADI and M. R. MOHAMMADI. Detecting ADHD children using symbolic dynamic of nonlinear features of EEG. In: *19th Iranian Conference on Electrical Engineering*. Tehran: IEEE, 2011, pp. 1–4. ISBN 978-964-463-428-4. DOI: 10.13140/RG.2.1.3306.1608.

[24] POLYCHRONAKI, G. E., P. Y. KTONAS, S. GATZONIS, A. SIATOUNI, P. A. ASVESTAS, H. TSEKOU, D. SAKAS and K. S. NIKITA. Comparison of fractal dimension estimation algorithms for epileptic seizure onset detection. *Journal of neural engineering*. 2010, vol. 7, no. 4, pp. 1–18. ISSN 1741-2560. DOI: 10.1088/1741-2560/7/4/046007.

[25] HIGUCHI, T. Approach to an irregular time series on the basis of the fractal theory. *Physica D: Nonlinear Phenomena*. 1988, vol. 31, no. 2, pp. 277–283. ISSN 0167-2789. DOI: 10.1016/0167-2789(88)90081-4.

[26] KATZ, M. J. Fractals and the analysis of waveforms. *Computers in Biology and Medicine*. 1988, vol. 18, no. 3, pp. 145–156. ISSN 0010-4825. DOI: 10.1016/0010-4825(88)90041-8.

[27] ESTELLER, R., G. VACHTSEVANOS, J. ECHAUZ and B. LITT. A comparison of waveform fractal dimension algorithms. *IEEE Transactions on Circuits and Systems I: Fundamental Theory and Applications*. 2001, vol. 48, no. 2, pp. 177–183. ISSN 1057-7122. DOI: 10.1109/81.904882.

[28] SEVCIK, C. A procedure to estimate the fractal dimension of waveforms. *Complexity International*. 1998, vol. 5, no. 1, pp. 1–19. ISSN 1320-0683.

[29] RAGHAVENDRA, B. S. and D. NARAYANA DUTT. Computing fractal dimension of signals using multiresolution box-counting method. *International Journal of Information and Mathematical Sciences*. 2010, vol. 6, no. 1, pp. 50–65. ISSN 2010-4065.

[30] HILBORN, R. C. *Chaos and Nonlinear Dynamics: An Introduction for Scientists and Engineers*. 2nd ed. Oxford: Oxford University Press, 2000. ISBN 978-0198507239.

[31] SANEI, S. *Adaptive processing of brain signals*. Oxford: John Wiley & Sons, 2013. ISBN 978-0-470-68613-3.

[32] OPPENHEIM, A. V., R. W. SCHAFER and J. R. BUCK. *Discrete-time Signal Processing*. 2nd ed. Upper Saddle River: Prentice Hall Englewood Cliffs, 1989. ISBN 0-13-754920-2.

[33] Hist3: Documentation. *MathWorks* [online]. 2017. Available at: `http://www.mathworks.com/help/stats/hist3.html?requestedDomain=se.mathworks.com`.

## About Authors

**Amin HEKMATMANESH** received his bachelor in Electrical Engineering from Science and Research of Fars University in 2010. His Master's degree was in Biomedical Engineering from Shahed University in Tehran, Iran 2013. His Masters thesis was about analyzing the Sleep EEG signal, Learning and Negative Emotional Memory. Since 2016 he is working as a researcher in the Laboratory of Intelligent machines in Lappeenranta University of Technology, Finland. His current research is about Brain Control Ankle Foot Orthosis Robot.

**Mohammad MIKAEILI** was born in 1968 in Mahabad, Iran. He received B.Sc. Degree in Electronics Engineering from Tehran University, Tehran, Iran, in 1989, and M.Sc. and Ph.D. Degrees in Biomedical Engineering from the Amirkabir University, Tehran, Iran, in 1994 and 2001, respectively. Since 2001, he has been with Shahed university, where he is currently an Assistant Professor at Engineering faculty. His current research interests include Biomedical signal processing, Sleep EEG analysis and BCI systems.

**Khosrow SADEGHNIIAT-HAGHIGHI** was born in 1964 in Iran. In 1993 he received Medical Doctor's (M.D.) degree and in 2001, Occupational Medicine specialty from Tehran University of Medical Sciences. He studied sleep medicine under supervision of Professor Shapiro from 2001 till 2002 in the University of Toronto. In 2005 he established the Iranian Sleep Medicine Society (ISMS) with the assistance of specialists in ENT, Neurology, Psychiatry, Occupational Medicine, pulmonology, pediatric and faciomandibular surgery. He also established two sleep clinics (Baharloo Sleep Clinic and Imam Sleep Lab) in Tehran University of Medical Sciences (2005), an Occupational Sleep Research center, and the first Sleep Medicine Fellowship educational center in Iran

(2013). He is also the head of the Environmental and Occupational Health Center, Ministry of Health and Medical Education and Editor-in-Chief of the Journal of Sleep Sciences.

**Huapeng WU** was born in 1964 in China, in 2001 he received Doctor of Science (Tech.) degree from Lappeenranta University of technology, Finland. He is an Associate Professor, 1.10.2004–current, and Professor, 01.01.2008–30.06.2011, in Lappeenranta University of Technology, Finland, his research interests include: robotics, AI control, Mechatronics, Mechanical Manufacturing & Automation, and publication include: 4 books, more than 100 publications in his research areas.

**Heikki HANDROOS** received his M.Sc. (Eng.) and D.Sc. (Tech.) degrees from Tampere University of Technology 1985 and 1991. He has been a professor of Machine Automation in Lappeenranta University of Technology since 1992. He has been a visiting professor in University of Minnesota, Peter the Great St Petersburg Polytechnic University and National Defense Academy (Japan). His research interests range from modelling, design and control of mechatronic transmissions to robotics and virtual engineering. He has published about 250 international scientific papers and supervised around 20 D.Sc. (Tech.) theses. He has been an Associate Editor of ASME Journal of Dynamic Systems, Measurement and Control since 2014. He has led several important domestic and international research projects.

**Radek MARTINEK** was born in 1984 in Czech Republic. In 2009 he received Master's degree in Information and Communication Technology from VSB–Technical University of Ostrava. Since 2012 he worked here as a Research Fellow. In 2014 he successfully defended his dissertation thesis titled "The Use of Complex Adaptive Methods of Signal Processing for Refining the Diagnostic Quality of the Abdominal Fetal Electrocardiogram". He became an Associate Professor in Technical Cybernetics in 2017 after defending the habilitation thesis titled "Design and Optimization of Adaptive Systems for Applications of Technical Cybernetics and Biomedical Engineering Based on Virtual Instrumentation". He works as an Associate Professor at VSB–Technical University of Ostrava since 2017. His current research interests include: Digital Signal Processing (Linear and Adaptive Filtering, Soft Computing - Artificial Intelligence and Adaptive Fuzzy Systems, Non-Adaptive Methods, Biological Signal Processing, Digital Processing of Speech Signals); Wireless Communications (Software-Defined Radio); Power Quality Improvement. He has more than 70 journal and conference articles in his research areas.

**Homer NAZERAN** holds B.Sc., M.Sc. and Ph.D. degrees in Electrical (Honors), Clinical and Biomedical Engineering from UT Austin, Case Western Reserve and University of Texas Southwestern Medical Center (UTSWM) at Dallas/UTA, respectively. He has close to 3 decades of experience in industry and academia and has practiced and taught biomedical engineering in the Middle East, Europe, Australia and USA. In Australia, with Professor Andrew Downing he co-founded the School of Engineering at the Flinders University of South Australia, introduced and established the electrical and electronics and biomedical engineering degree programs (1991 to 2001). He returned to the University of Texas at Arlington as a visiting professor in 1997 and 2001. He joined UTEP in 2002 to create and establish biomedical engineering degree programs at the Department of Electrical and Computer Engineering. His research interests are in the areas of computer modeling of physiological systems, intelligent biomedical instrumentation and biomedical signal processing as applied to chronic health conditions and telemedicine. He has more than 150 journal and conference articles in his research areas published in IEEE Engineering in Medicine and Biology Society (EMBS) and other flagship international conference proceedings. He is a reviewer for several national and international journals in his related fields including IEEE Transactions on Biomedical Engineering, Medical and Biological Engineering and Computing, Biomedical Engineering Online and others. His teaching interests are in electronics, biomedical instrumentation, physiological systems, and biomedical signal processing. He is also interested in development of novel teaching methods, lifelong learning and critical thinking habits in the classroom and interdisciplinary education based on application of nonlinear dynamics systems (complexity) theory. His research, teaching and professional activities have been supported by NIH, NSF, and DOE among others.